INNOVATIVE MECHANICAL ENGINEERING **ISSN 2812-9229 (Online)**
University of Niš, Faculty of Mechanical Engineering
VOL. 3, NO 3, 2024, PP. 20-29

Original scientific paper *

THE EFFECT OF WELDING SPEED ON THE MECHANICAL PROPERTIES OF FSW JOINTS IN AA2024-T351 ALUMINIUM ALLOY

Miodrag Milčić[1], Dragan Milčić[1], Nataša Zdravković[1], Natalija Mratinković[1]

[1]University of Niš, Faculty of Mechanical Engineering, Department of Mechanical constructions, development and engineering

Abstract. *To achieve high-quality friction stir welded (FSW) joints with reliable mechanical performance, it is essential to select appropriate welding parameters. This study investigates the effect of welding speed on the fracture toughness and impact strength of butt joints in AA2024-T351 aluminum alloy produced by FSW. The experiments were conducted using a constant tool rotation speed of 750 rpm and varying welding speeds of 73, 116, and 150 mm/min. Fracture toughness and impact strength were evaluated in distinct zones of the FSW joint, providing insight into the correlation between welding speed and mechanical properties.*

Key words: *Friction stir welding; Process parameters; Welding speed; Tool rotation speed; AA2024-T351; Fracture toughness; Impact strength*

1. INTRODUCTION

Wayne Thomas and his team of researchers at the Welding Institute (TWI) in the UK patented the Friction Stir Welding (FSW) process in 1991 as a solid-state joining technique, which was initially applied to aluminum alloys [1]. This innovative process has found extensive application, particularly in the automotive and aerospace industries for welding aluminum alloys that are challenging to weld using conventional methods. The FSW process offers superior mechanical properties in the joints compared to traditional techniques and requires less energy since it avoids melting the base material. Furthermore, it is an environmentally friendly technology that minimizes pollution. A notable advantage of this process is the minimal deformation observed when welding thin sheets of considerable length, a benefit unmatched by other welding methods.

FSW is predominantly employed for joining aluminum alloys, which pose difficulties when welded by traditional processes. The principle of achieving inseparable joints

*Received: December 15, 2024 / Accepted December 27, 2024.
Corresponding author: Miodrag Milčić
Institution: University of Niš, Faculty of Mechanical engineering
E-mail: miodrag.milcic@masfak.ni.ac.rs

through FSW is illustrated in Figure 1. This process utilizes a specialized tool to join the parts, proceeding through four distinct phases: 1) plunging phase, 2) dwelling phase, 3) welding phase, and 4) exit or retract phase [2].

The tool rotates around its axis while simultaneously moving axially relative to the base metal parts being joined. The primary functions of the tool are as follows:

- Pre-heating the base metal in the welding zone,
- Deforming and mixing the materials, and
- Creating the friction stir weld.

Pre-heating of the base metal is achieved through friction between the tool and the base metal, generating heat that facilitates the deformation and mixing of the base material into a monolithic joint. During the initial plunging phase, heating occurs primarily due to friction between the tool pin and the workpiece. The tool penetrates until the shoulder of the tool comes into contact with the workpiece. Once the plunging phase is completed, the tool continues to rotate, stabilizing the material and preparing it for the welding phase (dwelling phase).

As the tool pin rotates, the material of the workpieces is cut, deformed, and mixed with previously deformed material. The tool pin induces movement of parts of the base metal around the tool and towards its axis. During the tool's translational motion, deformed material is deposited in the zone behind the tool, thereby forming the weld joint (welding phase). The welding cycle concludes with the fourth phase, in which the tool exits the material vertically (Fig. 1).

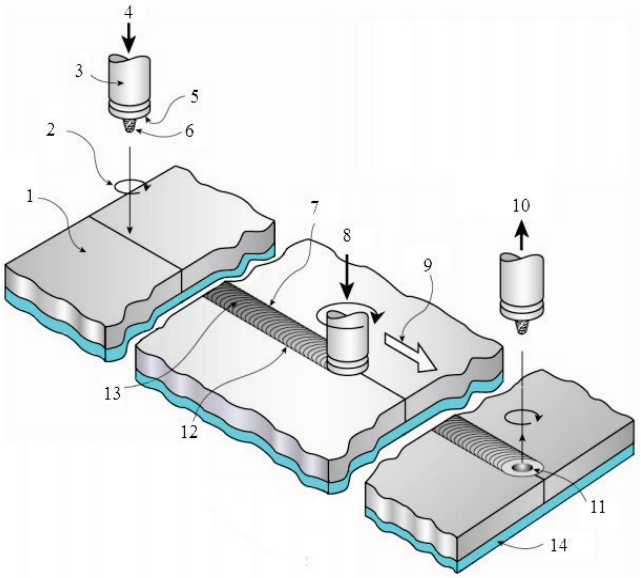

Fig. 1 Illustrated scheme of friction stir welding [3] (1 - base metal, 2 - direction of tool rotation, 3 - weld tool, 4 - downward movement of tool, 5 – tool shoulder, 6 – pin, 7 - advancing side of weld, 8 - axial force, 9 - direction of welding, 10 - upward movement of tool, 11 - exit hole, 12 - retreating side of weld, 13 - weld face and 14 - base plate)

Welding parameters, tool geometry, and joint design significantly influence material flow structure and temperature distribution, thereby affecting the microstructure development in the material. Two critical parameters for the FSW process are [4-8]:

1. The rotational speed of the tool (rpm), either in the clockwise or counterclockwise direction, and

2. The tool's translational speed along the joint line.

A distinctive feature of friction stir welds is the complex microstructure of the welded joint, which consists of different welding zones markedly different from the base metals being welded. The microstructure of FSW joints is heavily influenced by the tool's structural design, rotation speed, welding speed, tool pressure along the vertical axis, the angle at which the tool interacts with the material, and the properties of the material being welded. The microstructure of the welded joint can be divided into several zones: the heat-affected zone (HAZ), the thermo-mechanically affected zone (TMAZ), the nugget zone (NZ), and the base material [9-11].

It is crucial to select an appropriate combination of welding parameters to ensure a defect-free welded joint with the desired quality [12].

The primary objective of this research is to analyze the impact of key FSW parameters, specifically tool rotational speed and welding speed, on the structural and mechanical properties of FSW joints made from aluminum alloy AA2024-T351 [13].

2.EXPERIMENTAL PART

The experimental investigations aimed to evaluate the influence of the FSW process on the metallurgical and mechanical properties of welded joints. The base material used in this study was AlCu4Mg1 (AA2024-T351), an aluminum alloy known for its challenging weldability using conventional welding techniques. The chemical composition and mechanical properties of the base material are presented in Table 1 and Table 2.

Table 1 Chemical composition of AA2024-T351 base materials, data from [12].

Chemical Composition	Al	Cu	Mg	Mn	Fe	Si	Zn	Ti
wt. %	90.7–94.7	3.8–4.9	1.2–1.8	0.3–0.9	0.5	0.5	0.25	0.15

Table 2 Mechanical properties of AA2024-T351 base materials, data from [12].

Yield Strength Reh (Mpa)	Ultimate Tensile Strength Rm (MPa)	Elongation A5 (%)	Hardness HV
≥310	≥425	≥10	137

The dimensions of the welding samples were 500 mm in length, 65 mm in width, and 6 mm in thickness. An austenitic plate was placed beneath the welding samples to retain heat in the welded joint area. A conventional milling machine was utilized for the welding process, producing welds approximately 400 mm in length.

Fig. 2 illustrates the conventional milling machine used for welding and the tool employed for creating a butt FSW joint. The most critical parameters of the FSW process are the welding speed and the tool rotational speed.

a) b)

Fig. 2 Conventional Milling Machine for FSW (a) and FSW tool and tool geometry (b)

Experimental research was conducted with a constant tool rotational speed, while varying the welding speed, as shown in Table 3.

Table 3 Friction stir welding parameters.

Sample	Rotation speed n (rpm)	Welding speed v (mm/min)	Ratio n/v (rev/mm)
A		73	10,27
B	750	116	6,47
C		150	5

After completing the welding process, the welded joints were evaluated using non-destructive testing methods. Visual and radiographic inspections were performed on the samples, and no welding imperfections were detected.

Specimens for fracture toughness and Charpy impact testing were prepared with notches positioned at the center of the welded joint, as well as 4 mm away from the weld center on the advancing side (AS) and retreating side (RS) of the FSW joint (Figure 3a). Specimens for fracture toughness testing were extracted from the FSW welded samples, along with V-notched specimens at different positions within the FSW joint for Charpy pendulum impact testing. The dimensions of the specimens for both fracture toughness and Charpy impact testing are depicted in Figures 3b and 3c.

Fracture toughness of the FSW joint was evaluated on specimens prepared in accordance with the ASTM E1820 Standard [13], as illustrated in Figure 4b. The specimens had a thickness of 6 mm, and an initial notch (3.5 mm long and 0.5 mm wide) was created using Wire Electrical Discharge Machining (WEDM) technology. This notch served as a pre-crack seam for inducing a fatigue crack within the range of 5.4–6.6 mm using a Rumul Cracktronic device (Russenberger Prüfmaschinen AG, Neuhausen am Rheinfall, Switzerland) under pulsating loading (loading ratio R=0.1).

Impact toughness testing was performed using an instrumented Amsler RPK 300 pendulum at room temperature. Charpy impact toughness was determined using specimens measuring 5×10×55 mm, featuring a V-notch with a depth of 2 mm and a notch radius of 0.25 mm.

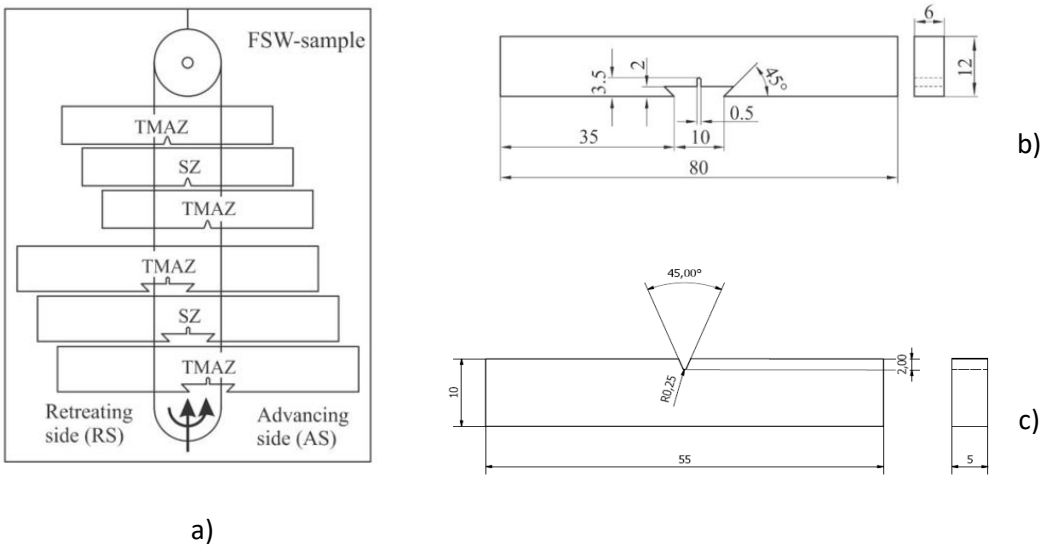

Fig. 3 Subtraction of the plate specimen for the fracture toughness testing and Sharpy impact test (a); Dimension of specimen for the fracture toughness testing (b); and Sharpy impact test specimens (c)

(TMAZ - notch position 4 mm from center of weld on advancing side (AS) and retreating side (RS); SZ - notch position in center of weld)

The length of the initial fatigue crack adhered to the guidelines specified in the ASTM E1820 Standard [13], meeting the condition $0.45 \leq a0/W \leq 0.55$, where W=12 mm for the specimen shown in Figure 4b. Prepared specimens were subjected to bending loading at room temperature on round supports spaced $S=4 \cdot W=4 \cdot 12=48$ mm apart, with the load applied at the midpoint on the side opposite the initial crack. Bending force and Crack Mouth Opening Displacement (CMOD) were recorded until specimen failure, as prescribed by the ASTM E1820 Standard [13] (Fig. 4b).

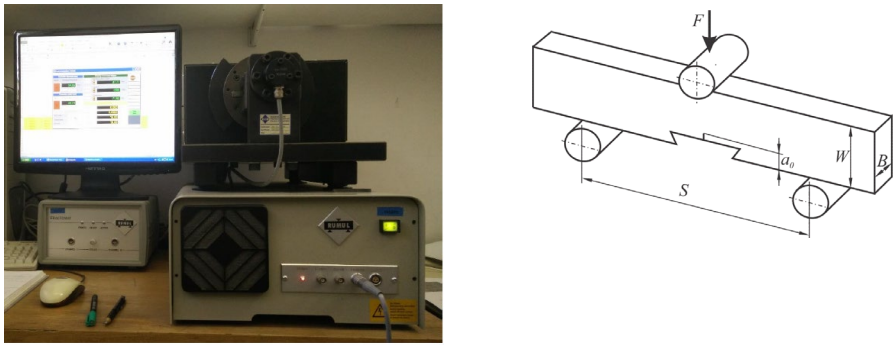

Fig. 4 Fracture toughness testing setup on a Rumul Cracktronic (a); bend test fixture design (b). (Specimen: B - width; W – height; a0 – initial crack size; S – support distance; F - load)

3. RESULTS

Table 4 presents the F−t and E−t diagrams for specimens with notches located at the weld center from welded samples A, B, and C.

Table 4 Friction stir welding parameters.

A-SZ	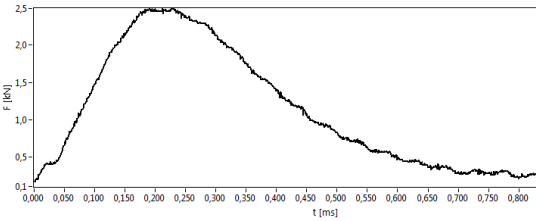	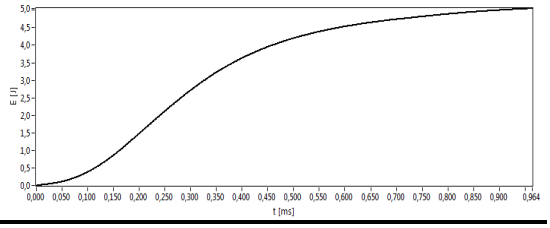
B-SZ	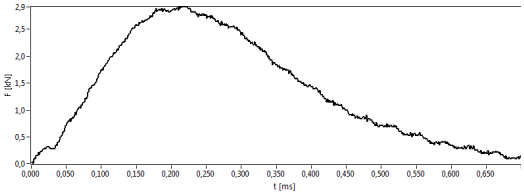	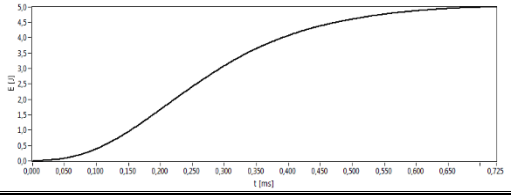
C-SZ	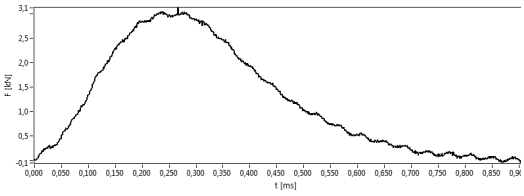	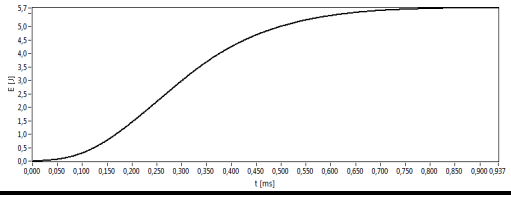

Table 5 Impact energy of welded specimens: crack initiation, crack propagation, and overall impact energy.

Simple	E / J	E_i / J	E_p/ J	KV / J/cm^2
BM	7.8	3	4.8	19.5
A-SZ	5,05	1.64	3.41	12.62
A-AS	6.8	3	3.8	17.1
A-RS	5.5	2.1	3.4	13.6
B-SZ	6.7	1.7	5	12.62
B-AS	8.5	3.2	5.3	21.3
B-RS	4.5	1.4	3.1	11.1
C-SZ	5.7	2.4	3.3	14.2
C-AS	8.3	3.1	5.2	20.7
C-RS	5.1	1.9	3.2	12.8

The measured impact energy values were low, below 10 J, indicating that the welded joints exhibit brittle behavior. For all welded specimens, the maximum impact energy values were observed on the advancing side of the welded joint. The highest impact energy, 8.5 J, was recorded for samples welded with parameters n=750 rpm, and a welding speed of 116 mm/min, with the notch positioned on the advancing side.

Similar to the base metal (Table 4), the crack propagation energy values exceeded the crack initiation energy values (Fig. 5). Among all the welded samples, the lowest impact energy was observed in specimens with a notch positioned on the retreating side.

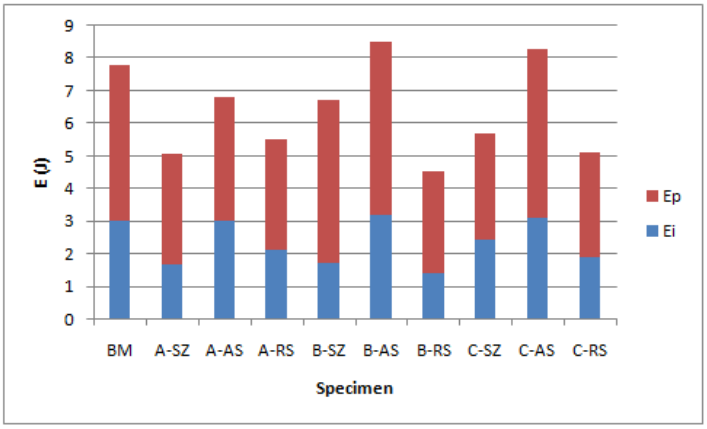

Fig.5 Impact energy of welded specimens: crack initiation, crack propagation, and overall impact energy

After testing, the specimens were subjected to a temperature of 200 °C to oxidize the crack surfaces, facilitating improved visualization of the remaining ligament (Fig. 6).

Critical J-integral values (J_{IC}) for different structures of welded joints were obtained at varying welding speeds. These critical values were determined according to the ASTM E1820 Standard and are presented in Table 6. The fracture toughness K_{JIc} was calculated using the following expression:

$$K_{JIc} = \sqrt{\frac{E \cdot J_{Ic}}{1-\nu^2}} \tag{1}$$

where:

- v—Poisson's ratio,
- E—modulus of elasticity (MPa).

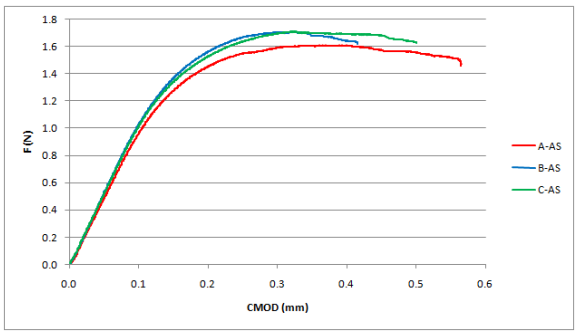

a)

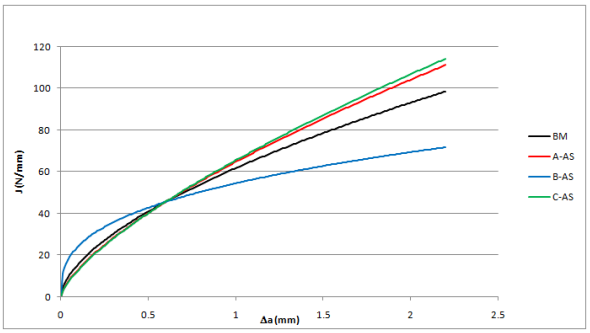

b)

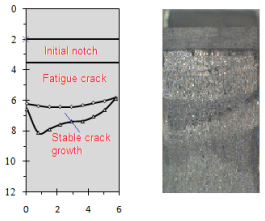

c)

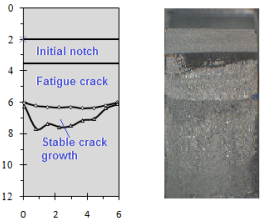

d)

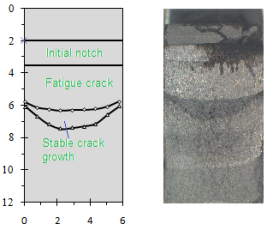

e)

Fig.6 (a) Experimental data of load-displacement for specimens A-AS, B-AS and C-AS; (b) Comparisons of J-R curves for specimen A-AS, B-AS and C-AS; (c) crack surfaces on advancing side for specimen A-AS; (d) crack surfaces on advancing side for specimen B-AS; (e) crack surfaces on advancing side for specimen C-AS.

Table 6 Fracture toughness K_{JIc} of the analyzed FSW joint for different welding speeds and notch locations [14, 15].

Sample	J_{Ic} N/mm	K_{JIc} N/m$^{3/2}$
BM	27	47
A-AS	25	45.3
A-RS	29	48.8
B-AS	33.5	52.4
B-SZ	23	43
B-RS	39	56.5
C-AS	24.6	44.9
C-SZ	23	43.4
C-RS	28	47.9

Analysis of the fracture toughness results indicates that, for all welding samples, the structure of the welded joint on the retreating side exhibits the highest fracture toughness (Figure 7). This suggests that the retreating side has greater resistance to crack propagation compared to the structure on the advancing side in all tested samples.

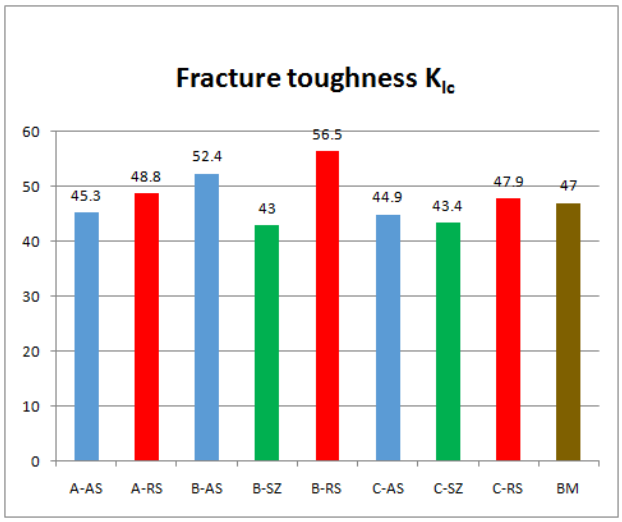

Fig.7 Fracture toughness values K_{Ic} for welded joints achieved by different welding parameters and different notch positions.

4. CONCLUSION

The research presented in this paper investigated the fracture behavior of FSW-AA2024-T351 joints, which are commonly used in lightweight aerospace structures. Friction stir welding (FSW) is a joining process where the mechanical and structural properties of the welded joint depend on numerous interrelated welding parameters. This study focused on analyzing the effect of welding speed on the fracture behavior of FSW-AA2024-T351. Based on comprehensive experimental testing and fracture analysis at three different welding speeds (v=73,116 and 150 mm/min) with a constant rotation speed of n=750 rpm, the following conclusions can be drawn:

- The relationship between tool rotational speed (n) and welding speed (v) directly affects fracture toughness and the energy required for crack initiation and propagation.
- The highest impact energy values were observed in samples welded at n=750 rpm and a welding speed of v=116 mm/min, with the notch positioned on the advancing side (B+4).
- Analysis of fracture toughness results shows that the welded joint structure on the retreating side consistently exhibits higher fracture toughness, demonstrating greater resistance to crack propagation compared to the advancing side in all tested samples.
- Comparing fracture toughness of joints produced with different welding parameters at the same notch position, the highest fracture toughness was observed in joints welded with parameters B−750/116, followed by joints welded with A−750/73 and C−750/150. The latter two showed approximately 15% lower fracture toughness.

REFERENCES

1. Thomas W M, Nicholas E D, Needham J C, Murch M G, Temple-Smith P, Dawes C J 1991 Friction stir butt welding, GB Patent No. 9125978.8, International patent application No. PCT/GB92/02203.
2. Gupta R K, Das H and Pal T K 2012 Influence of Processing Parameters on Induced Energy, Mechanical and Corrosion Properties of FSW Butt Joint of 7475 AA, JMEPEG 21, pp.1645–1654
3. Su J Q, Nelson T W, Mishra R, and Mahoney M 2003 Microstructural Investigation of Friction Stir Welded 7050-T651 alloy, Acta Mater., 51, pp. 713–729
4. Ma Z Y and Mishra R S 2005 Friction stir welding and processing, Materials science and engineering", vol. 1, no. 1, pp. 1-78.
5. Zimmer S, Langlois L, Laye J and, Bigot R 2010 Experimental investigation of the influence of the FSW plunge processing parameters on the maximum generated force and torque, Int J Adv Manuf Technol 47, pp.201–215.
6. Hussain K 2010 Evaluation of parameters of friction stir welding for aluminium AA6351 alloy, International journal of engineering science and technology, vol. 2, no. 10, pp. 5977-5984.
7. Ouyang J, Yarrapareddy E and Kovacevic R 2006 Microstructural evolution in the friction stir welded 6061 aluminum alloy (T6-temper condition) to copper, Journal of Materials Processing Technology, 172, pp 110–122.
8. AWS D17.3/D17.3M: 200x Specification for Friction Stir Welding of Aluminium Alloys for Aerospace Hardware, An American National Standard, American Welding Society/ Miami, Florida, January 2010, p. 60.
9. Radisavljević I, Živković A, Grabulov V and Radović N 2015 Influence of pin geometry on mechanical and structural properties of butt friction stir welded 2024-T351 aluminum alloy, Hem. Ind. 69 (3), pp.323–330
10. Perović M, Baloš S, Kozak D, Bajić D and Vuherer T 2017 Influence of kinematic factors of friction stir welding on the characteristics of welded joints of forged plates made of EN AW 7049 a aluminium alloy, Tehnical gazette 24, 3, pp.723-728.
11. Vilaça P, Mendes J, Nascimento F and Quintino L, 2016 Application of FSW to Join Aluminium Foil Winding Coils for Electrical Transformers, Int J Mech Syst Eng, Volume 2. 2016. 115, doi:10.15344/2455-7412/2016/115
12. Alcoa. Alloy 2024 Sheet and Plate. Available online: http://www.matweb.com/search/datasheet_print.aspx?matguid=67d8cd7c00a04ba29b618484f7ff7524 (accessed on 20 February 2021).
13. ASTM E1820. Standard Test Method for Measurement of Fracture Toughness; ASTM International: West Conshohocken, PA, USA, 2015.
14. Milčić, M.; Milčić, D.; Vuherer, T.; Radović, L.; Radisavljević, I.; Đurić, A. Influence of Welding Speed on Fracture Toughness of Friction Stir Welded AA2024-T351 Joints. Materials 2021, 14, 1561. https://doi.org/10.3390/ma14061561
15. Milčić M., 2020, Research on influence of the friction stir welding's parameters on weelded joint's fatigue strength at AA 2024 T351, Doctoral disrtation, University of Niš, faculty of Mechanical Engineering, Niš.